Evaluation of the Multipath Characteristics of the Impulse Radio Channel

R. Jean-Marc Cramer*, Moe Z. Win†, and Robert A. Scholtz*
*Communication Sciences Institute, EEB 500
Department of Electrical Engineering - Systems
University of Southern California, Los Angeles, CA 90089-2565 USA
†Wireless Systems Research Department
Newman Springs Laboratory, AT&T Labs-Research
NSL 4-147, 100 Schulz Dr., Red Bank, NJ 07701-7033 USA

Abstract— **In order to estimate performance of impulse radio communication systems, a characterization of the channel is required. In particular, knowledge of the multipath angle and time-of-arrival distributions is useful for predicting the performance of diversity reception schemes. In this paper, the CLEAN algorithm is applied to ultra-wide bandwidth (UWB) signals received on an array of sensors in order to resolve the incident signal components.**

I. Introduction

Techniques for generating ultra-wide bandwidth (UWB) or "baseband carrierless short pulse" signals have been in existence for more than three decades [1], with primary utility in the radar community. A comprehensive reference of early work in this area can be found in the paper by Bennett and Ross [2]. More recently, UWB signals have been considered for application in communication systems, in particular spread-spectrum communications, in part because of the fine time resolution afforded by these signals [7], [8]. These time resolution properties make UWB radio a candidate for short range communications in dense multipath environments [9], [10]. In order to gain a more complete understanding of this potential, an accurate model of the propagation characteristics of the transmitted waveforms is required. In particular, the existence of multipath components arriving at the receiver with different time delays and from different directions can create a dynamic and extended channel impulse response. Characterization of the propagation channel may therefore influence the design of Rake receiver diversity algorithms for this channel. A goal of this work is to develop channel models on which spatio-temporal algorithms for UWB communication systems can be tested with confidence. Implicit in this is an understanding of the distortions experienced along individual propagation paths.

This paper presents the results of delay-and-sum beamforming, applied to ideal UWB signals and to measured UWB propagation data taken on an array of sensors at different locations within an office building. The potential of the CLEAN algorithm is demonstrated in resolving simulated UWB signals. In particular, the dynamic range and angular resolution performance is shown.

A bandwidth measure for UWB signals can be defined by the fractional bandwidth B_f as [3],

$$B_f = 2\frac{f_H - f_L}{f_H + f_L} \tag{1}$$

where f_H and f_L are the upper and lower 3 dB points of the signal spectrum, respectively. UWB signals are defined as having a fractional bandwidth greater than 25% [3], [4].

II. Impulse Radio Fundamentals

The theoretical performance of UWB impulse radio communication systems has been investigated in the absence of degradations due to multipath interference [5], [6], [7], [8]. The information bearing signal associated with impulse radio is a time-hopped, pulse-position modulated signal, given for the k^{th} transmitter by

$$s_{tr}^{(k)}\left(t^{(k)}\right) = \sum_{j=-\infty}^{\infty} w_{tr}\left(t^{(k)} - jT_f - c_j^{(k)}T_c - d_j^{(k)}\right) \tag{2}$$

where $t^{(k)}$ represents the transmitters' clock time, and $w_{tr}(t)$ represents the transmitted waveform. The transmission frame time is given by T_f and the unique time-hopping sequence or code assigned to the k^{th} user is given by $\left\{c_j^{(k)}\right\}$. The parameter T_c is the duration of an addressable time bin. The sequence $\left\{d_j^{(k)}\right\}$ is determined from the data sequence, with many pulses (values of j) used to represent one data symbol. Both multiple-access addressing via distinct hopping patterns and information are encoded in time-shifts relative to the frame clock.

The ideally modeled pulse shape propagating in free space is the first derivative of the Gaussian pulse generated by the transmitter. The response of the receive antenna to this ideal pulse is given by the second derivative Gaussian

This work was supported in part by the Integrated Media Systems Center at the University of Southern California, in part by the Joint Services Electronics Program under contract F49620-94-022 and in part by TRW Space and Electronics Group.

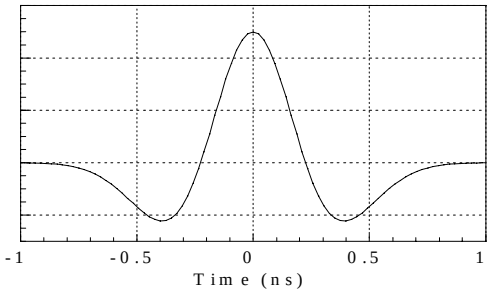

Fig. 1. Ideal impulse signal at output of receiver antenna for $\tau_m = 0.8$ ns.

waveform,

$$s_{rec}(t) = \left[1 - 4\pi\left(\frac{t-t_d}{\tau_m}\right)^2\right]\exp\left[-2\pi\left(\frac{t-t_d}{\tau_m}\right)^2\right], \tag{3}$$

where t_d represents the location of the pulse center in time and τ_m is a parameter which determines the temporal width of the pulse, and is approximately 0.8 nanoseconds (ns) in this work. This ideal signal is shown in Figure 1.

III. UWB Propagation Experiment

A UWB signal propagation experiment was performed in an office building by sounding the channel with the UWB waveforms [9]. Signal propagation measurements were made from a fixed impulse transmitter location to 14 different rooms and hallways of the office building, transmitting a pulse train of duty cycle 0.2% and of period of 500 nanoseconds. In each room, measurements over a window of 300 nanoseconds were made at 49 different locations arranged spatially in a fixed-height, 7 sensor $\times$ 7 sensor square grid with 6 inch inter-sensor spacing, shown in Figure 2. In this figure, θ represents the azimuth look direction. The elevation look angle is measured from perpendicular to the array. The same absolute delay reference for all recorded profiles was used. Typical measured high SNR profiles are shown in Figure 3, 4 and 5 for three different sensors located along a diagonal of the array. Based on the array geometry, this collection of measurements suggests an arrival direction for the direct path (leading edge of the data).

IV. Beamforming with Ultra-Wide Bandwidth Signals.

Given the bandwidth extent of the UWB signals, a delay-and-sum beamformer is used to process the received array of signals. Let the beamformer output for a planar array of sensors steered to an azimuth angle of θ and an elevation angle of ϕ, on incidence of a plane wave from an azimuth angle of θ_o and an elevation angle of ϕ_o, be represented by [3],

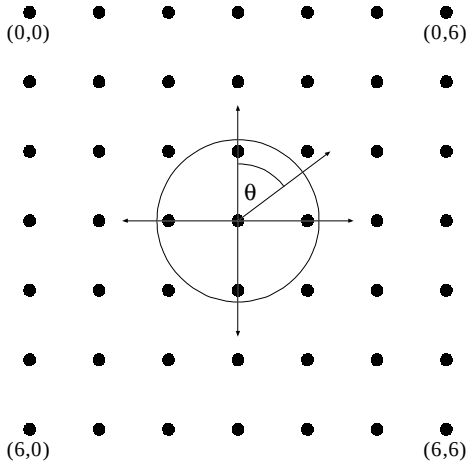

Fig. 2. Geometry and indexing of the array on which UWB signal propagation measurements were made.

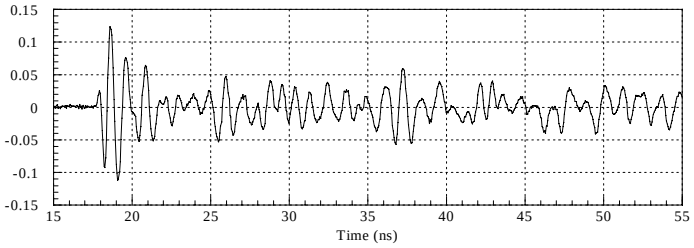

Fig. 3. Measured amplitude vs. time at sensor (0,6).

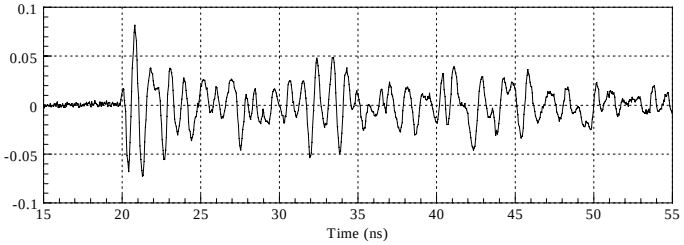

Fig. 4. Measured amplitude vs. time at sensor (3,3).

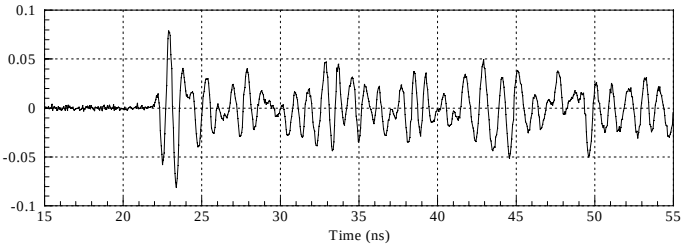

Fig. 5. Measured amplitude vs. time at sensor (6,0).

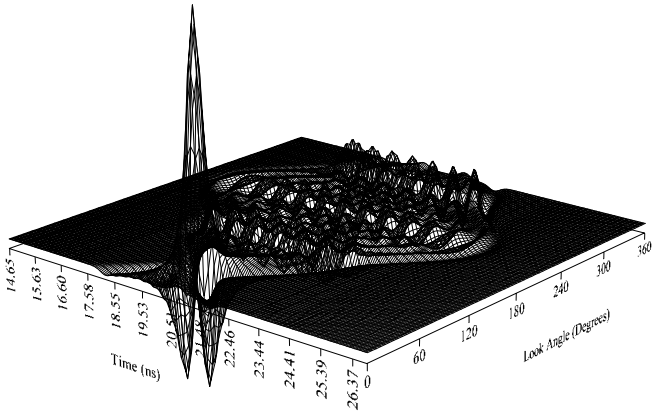

Fig. 6. Beamformer response to the ideal signal (3) vs. time and azimuth look angle at 90^o elevation, for the 49 element planar array with $s_{rec}(t)$ incident at an azimuth angle of 45^o and 90^o elevation.

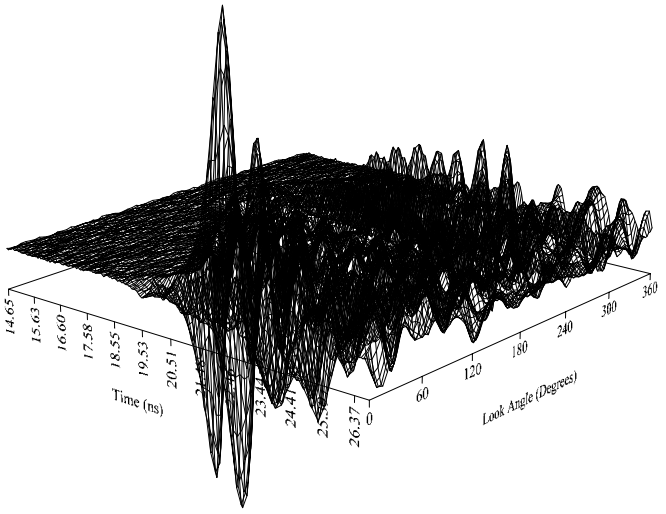

Fig. 7. Beamformer response to measured data for a "high SNR" case at 90^o elevation, between rooms in an office building.

$$B(\theta,\phi,t) = \sum_{m,n} a_{m,n}(\theta,\phi) \times$$
$$s_{rec}\left(t - (M-m)\frac{d_x}{c}(u-u_o) - (n-N)\frac{d_y}{c}(v-v_o)\right) \quad (4)$$

where $u = \sin\theta\sin\phi$, $v = \cos\theta\sin\phi$, $u_o = \sin\theta_o\sin\phi_o$, $v_o = \cos\theta_o\sin\phi_o$, d_x and d_y represent the inter-element spacings in the x and y-directions, respectively, and $a_{m,n}(\theta,\phi)$ is the antenna pattern of the element at position (md_x, nd_y) in the array. All time-shifts are referenced to the array geometric center at (Md_x, Nd_y). It is assumed here that each element has an isotropic pattern. Just as the expression for the array factor in the narrowband case is dependent on the assumed sinusoidal signal characteristics, this expression also explicitly depends on the received pulse shape. Distinct from the ideal narrowband case, it is seen in (4) that the beamformer can impart distortions to the received signal as it is steered away from the actual angle-of-arrival.

The response of the array in Figure 2 to $s_{rec}(t)$ of Figure 1 is given in Figure 6. The delay-and-sum beamformer was applied to measured data as well, and one case containing a pulse with arrival angle similar to that in Figure 6 is shown in Figure 7. Other signal components are present in this case, but are not as easily distinguishable.

Another plot of the beamformer output, where the time dependence has been removed, and the maximum amplitude at each look direction is recorded, is given in Figure 8 for the beamformer output of Figure 6. UWB array performance is governed by the sidelobe level of the beamformer and the ability to resolve closely spaced sources. The maximum sidelobe level of a UWB array is determined by the number of sensors that can add coherently at any off-peak look direction. Sidelobes with amplitude of nearly 1/7 that of the main beam appear in Figure 8, corresponding to the coherent addition of a row, column or diagonal of the array. The dynamic range of this beamformer in the absence of any post-processing is therefore limited by these sidelobes to approximately $20\log_{10}(7/1)$ or 16.9 dB. The resolution capability of the array is a function of both the temporal and angular separation of the incident UWB signals. Ignoring elevation angle, sources co-incident in time with an azimuth angular separation of less than $c\tau/L$ radians are not resolved, by assumption, without further processing [3]. Here τ is the time duration of the pulse, c is the speed of light and L is the length of the array. For the array geometry utilized here and ideal signals with τ_m=0.8 ns, this corresponds to an azimuth angular separation of roughly 15^o. These limitations are fundamental to interpretation of the measured data and suggest continued research on UWB array design and post-processing algorithms.

V. Channel Characterization

The goal of a channel characterization in this context is to extract the structure of the channel from the received data. Define the channel model for impulse radio communications to be

$$r(t) = \sum_{k=1}^{N} A_k s_{rec,k}(t - \tau_k, \theta_k, \phi_k) + n(t) \quad (5)$$

where τ_k is the time-of-arrival of the k^{th} out of N components, at an azimuth angle of θ_k degrees and an elevation angle of ϕ_k degrees. The received impulse waveform, $s_{rec,k}(t)$ depends on the index k, due to variations in the received signal shape. This dictates that the algorithm

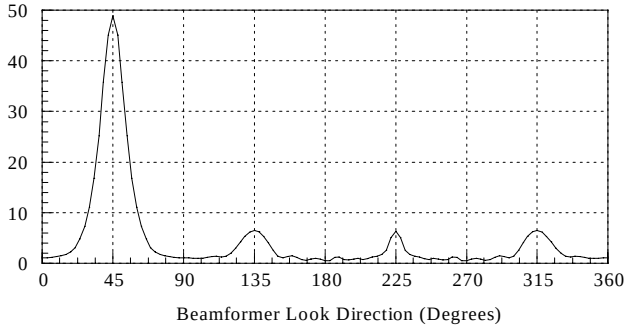

Fig. 8. Maximum projection for the 49 element array on incidence from an azimuth of 45^o and an elevation of 90^o.

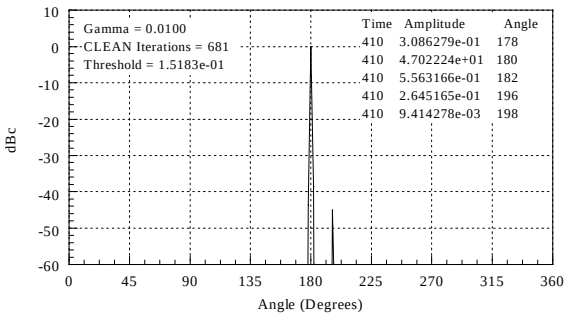

Fig. 9. CLEAN beam for two signals with a 40 dB difference in signal level.

should estimate $s_{rec,k}(t)$ from the received data. The technique proposed here for evaluation of the UWB channel is the CLEAN algorithm, introduced in [13] for the enhancement of radio astronomical maps of the sky. The algorithm has also found utility in the microwave and radar imaging communities [12], [14], for the reduction of antenna sidelobes. Use of the CLEAN algorithm here involves a variable array response with extent both in time and space. Modifications were therefore made, allowing estimation of the array response from the beamformer output. The steps in this modified CLEAN algorithm are as follows:

1. Generate the beamformer response to the input data over a window in time and angle.
2. Search the beamformer output window over time and angle for the peak response.
3. Determine and store the amplitude, time and angle-of-arrival of this peak response.
4. Estimate the signal corresponding to the peak response and store this waveform.
5. Generate the beamformer response to this estimated waveform.
6. Update the beamformer response by subtracting a fraction γ of the response to the estimated signal from the previous beamformer response,

$$B_n(\theta,t) = B_{n-1}(\theta,t) - \gamma \hat{B}_{k,n-1}(\theta,t) \qquad (6)$$

where,

k is an index of the largest response in $B_{n-1}(\theta,t)$.

$B_n(\theta,t)$ is the beamformer response at the n^{th} iteration.

$\hat{B}_{k,n-1}(\theta,t)$ is the estimated response to the k^{th} impulse at time $n-1$.

7. Add the current signal amplitude, scaled by γ, to the appropriate place in a list of signal locations.
8. If a stopping criterion (a threshold on the signal level or residual energy) is not met, go to step 2.
9. Generate a list of the signals found, including amplitude and the time and angle-of-arrival.
10. Form the CLEAN map by convolving the list of signals with delta functions.

CLEAN has been characterized using simulated impulse radio waveforms to define its performance limits. The ability to identify impulses which are coincident in time, with

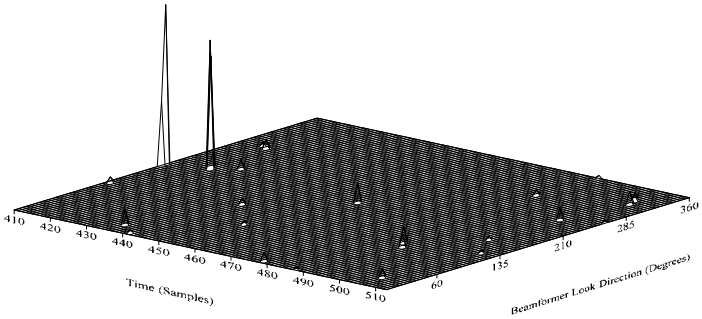

Fig. 10. CLEAN map for two signals in noise.

spatial separation equal to the angular resolution limit, both for equi-amplitude signals and those with an amplitude difference of 40 dB, was demonstrated. This is a significant improvement in the dynamic range, and the output of the algorithm is shown in Figure 9 for 2^o of angular quantization. Note that the ability of the algorithm to resolve closely spaced sources is a function of both the angular and temporal separation of the sources. The performance of the algorithm was also tested in the presence of noise. A typical CLEAN map for a moderate SNR, in the presence of two impulses separated in time by 0.5 ns (10 samples) and in azimuth angle by 10^o, is shown in Figure 10.

The CLEAN algorithm has been applied to measured data as well, under the assumptions of plane-wave incidence and an elevation angle-of-incidence of 90^o. The output of the algorithm, upon input of the measured data of Figure 7, is shown in Figure 11.

Current work includes the development of a theory for the selection of the loop gain and stopping criterion. Efficient methods of accounting for wavefront curvature and sensor position errors are also under investigation, as are improved array geometries for future measurements.

VI. Conclusion

An overview of impulse radio and UWB array signal processing was given and some of the current problems were

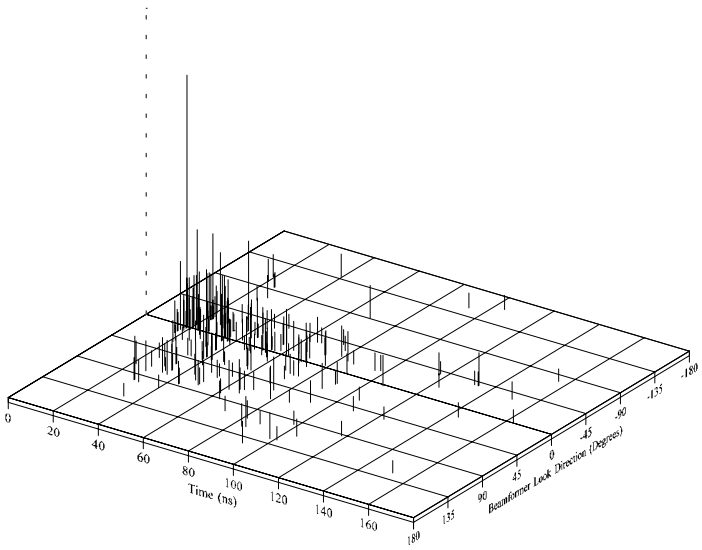

Fig. 11. Output of CLEAN algorithm upon input of high SNR data

outlined. A variant of the CLEAN algorithm was introduced as a potential means of extracting the channel model. The goal of this research is to develop an algorithm capable of characterizing the indoor UWB channel, and apply it to measured data taken in the channel. The final result should be a statistical characterization of typical UWB indoor propagation channels. This model may then be utilized in the design of UWB communication systems.

References

[1] G. F. Ross, "The transient analysis of certain TEM mode four-post networks," *IEEE Trans. Microwave Theory Tech.*, vol. MTT-14, p. 528, Nov. 1966.

[2] C. L. Bennett and G. F. Ross, "Time-domain electromagnetics and its applications," *Proc. IEEE*, vol. 66, pp. 299–318, Mar. 1978.

[3] J.D. Taylor, *Introduction to Ultra-Wideband Radar Systems*, CRC Press, Boca Raton, FL, 1995

[4] OSD/DARPA, *Ultra-Wideband Radar Review Panel, Assessment of Ultra-Wideband (UWB) Technology*, DARPA, Arlington, VA, 1990.

[5] R. A. Scholtz and M.Z. Win, "Impulse Radio", *Personal Indoor Mobile Radio Conference*, Helsinki, Finland, Sept. 1997, Printed in *Wireless Communications: TDMA vs. CDMA*, S.G. Glisic and P.A. Leppänen, eds., Kluwer Academic Publishers, 1997.

[6] R.A. Scholtz, "Multiple Access with Time-Hopping Impulse Modulation," in *Proc. Milcom*, Oct. 1993.

[7] M. Z. Win and R. A. Scholtz, "Impulse radio: How it works," *IEEE Commun. Lett.*, Feb. 1998.

[8] M. Z. Win and R. A. Scholtz, "Comparisons of analog and digital impulse radio for multiple-access communications," in *Proc. IEEE Int. Conf. on Comm.,* pp. 91–95, June 1997. Montréal, Canada.

[9] M. Z. Win, R. A. Scholtz, and M. A. Barnes, "Ultra-wide bandwidth signal propagation for indoor wireless communications," in *Proc. IEEE Int. Conf. on Comm.*, pp. 56–60, June 1997. Montréal, Canada.

[10] M. Z. Win and R. A. Scholtz, "On the robustness of ultra-wide bandwidth signals in dense multipath environments," *IEEE Commun. Lett.*, vol. 2, no. 2, pp. 51-53, Feb. 1998.

[11] J. G. Proakis, *Digital Communications.* McGraw-Hill, Inc., third ed., 1995.

[12] J. Tsao and B.D. Steinberg, "Reduction of Sidelobe and Speckle Artifacts in Microwave Imaging: The CLEAN Technique", *IEEE Trans. on Antennas and Prop.*, vol. 36, No. 4, April, 1988.

[13] J.A. Högbom, "Aperture Synthesis with a Non-Regular Distribution of Interferometer Baselines", *Astron. and Astrophys. Suppl. Ser.*, vol. 15, p.417-426, 1974.

[14] Q. Spencer, M. Rice, B. Jeffs, M. Jensen, "Indoor Wideband Time/Angle of Arrival Multipath Propagation Results", *IEEE Vehicular Technology Conference*, IEEE, 1997, p. 1410-1414.